Hydrol. Earth Syst. Sci. Discuss., 5, 1677–1704, 2008
www.hydrol-earth-syst-sci-discuss.net/5/1677/2008/
© Author(s) 2008. This work is distributed under
the Creative Commons Attribution 3.0 License.

Hydrology and Earth System Sciences Discussions

Papers published in *Hydrology and Earth System Sciences Discussions* are under open-access review for the journal *Hydrology and Earth System Sciences*

Modelling dominant runoff production processes at the micro-scale – a GIS-based and a statistical approach

C. Müller[1], H. Hellebrand[2], M. Seeger[3], and S. Schobel[4]

[1]University of Trier, Department of Soil Sciences, Trier, Germany
[2]Delft University of Technology, Department of Civil Engineering and Geosciences, Department of Watermanagement, Section of Hydrology, Delft, The Netherlands
[3]University of Trier, Department of Physical Geography, Trier, Germany
[4]Johann Heinrich von Thünen-Institute, Institute of Forest Ecology and Forest Inventory, Eberswalde, Germany

Received: 3 June 2008 – Accepted: 11 June 2008 – Published: 30 June 2008

Correspondence to: C. Müller (cmueller@uni-trier.de)

Published by Copernicus Publications on behalf of the European Geosciences Union.

Abstract

In this study two approaches are presented to model Dominant Runoff production Processes (DRP) with respect to regionalization. The approaches have been developed in the micro-scale experimental Zemmer basin (Germany). The first approach combines the permeability of the substratum, land-use and slope of the basin in a GIS-based analysis. The second approach makes use of discriminant analysis of the physiographic characteristics of the basin and links it to the GIS analysis. The net results were two maps indicating modelled DRP for the Zemmer basin, which were then compared to an existing DRP map of the Zemmer basin. Both approaches provided satisfactory results when compared to this existing DRP map. The first approach was strongly linked to the geological conditions of the basin while the second approach revealed a strong dependence on the topography. Therefore, impermeability of the substratum and the topography of the basin were used as suitable parameters for modelling dominant runoff processes.

1 Introduction

Several aspects of runoff formation have been studied in micro-scale basins over the past years (e.g. Anderson and Burt, 1990; Buttle and McDonald, 2002; McDonnell, 2003; Scherrer et al., 2006; Scherrer, 1997; Weiler et al., 2005; Weiler and Naef, 2003). At the micro-scale (i.e. basins ranging in size from 1 km^2 to 10 km^2; Blöschl, 1996) runoff generation processes occurring at hill slopes and near-stream areas dominate basin response to rainfall (McDonnell, 1990; Montgomery, et al., 1997). In many cases several processes were observed to occur simultaneously at the same site, however, during prolonged precipitation often one process tends to dominate so that other processes can be neglected (Scherrer and Naef 2001). Methods to identify the runoff processes on the plot scale have been developed for example by Peschke et al. (1999), Scherrer (1997) and Faeh (1997). Scherrer (1997) and Faeh (1997) conducted sprinkling experiments in Switzerland on grassland hill slopes with varying slopes, geology and soils, recording soil-water level, soil-water content and soil-water tension. The outcome of this research formed the basis for developing process decision schemes, which reflect the complex nature of runoff formation eventually to determine the Dominating Runoff producing Process (DRP) on a soil profile (Scherrer and Naef, 2003). The processes thus derived are: Hortonian Overland Flow (D_{HOF}), Saturated Overland Flow (D_{SOF}), SubSurface Flow (D_{SSF}) and Deep Percolation (D_{DP}). The SOF and SSF processes are subdivided into D_{SOF1}, D_{SOF2} and D_{SOF3} and D_{SSF1}, D_{SSF2} and D_{SSF3} respectively. The numbers refer to the intensity with which the processes react to rainfall, where 1 represents, relatively seen, the most abruptly changing flow reaction and 3 represents the most gradually changing flow reaction. However, this approach is time consuming and more often than not, detailed soil data such as soil- and drainage maps are not available making it difficult to be applied on a smaller scale. Schmocker-Fackel et al. (2007) simplified the complex decision scheme of Scherrer and Naef (2003) but still requires data from detailed soil maps (1:5000) and from geological, land-use and topographical maps. The problems connected with this approach are well known, because normally such detailed soil maps are non-existent.

A combination of GIS-based data and the permeability of the substratum circumvent the use of detailed soil maps for the regionalization of the above-described DRPs. In a study of winter storm flow coefficients and their generation Hellebrand et al. (2007) proved that the permeability of the substratum can very well be used with regard to dominant runoff production processes. Moreover statistical analysis of DRPs and basin characteristics could provide insight into regionalization opportunities without using detailed soil maps. Since soil relief parameters are determinant for soil formation and for runoff generation (Ticehurst et al., 2007), they are considered as crucial for soil and process mapping purposes. Besides other statistical and computational methods, discriminant analysis has been widely used to differentiate and characterise different spatial and soil process units (Kravchenko et al., 2002; Sinowski and Auerswald, 1999). One of the most important advantages of this linear statistical approach is the fact that all developed parameters are interpretable with parameters derived from known data. With this, it is possible to identify and quantify the differences and similarities of areas with common (hydrological) behaviour.

The objective of this study is to develop two different models for regionalization of dominant runoff processes: (i) a simple GIS-based procedure based on slope and permeability of the substratum and (ii) a stratified statistical model based on a discriminant analysis of a large set of GIS-based derivates. In order to determine the validity of both approaches, their results will be compared to an existing reference map (Schobel, 2005), which reflects the dominant runoff processes of the study area.

2 Study area

The study area consists of the micro-scale experimental Zemmer basin located in Rhineland-Palatinate, Germany. Its physiographic basin characteristics, namely land-use, permeability of the substratum and slope are given in Table 1. The research area of the Zemmer basin (Fig. 1) comprises the sub-basins of the Grundsgraben basin and the Schleidweiler basin, situated in the southern part of the Eifel near the village of Zemmer.

The municipality of Zemmer consists of four small towns, three of which are situated on a plateau. The fourth sub-municipality lies in the "Kyll" valley and was subjected to repeat flooding in the past. Mesozoic sediments of the formations sandstone and limestone form thin surface layers covering the bedrock of Devonian schist. In higher elevated areas, this pattern is covered by tertiary sediments of the Ur-Mosel (ranging from yellow- red- brownish clays to sandy sediments and pebble) as well as by Pleistocene solifluctional cover and swayed by loess (Walter, 1995). The in-situ loamy-sandy to loamy-clayey as well as clayey weathered rock of the upper sandstone (so1 and so2) led to the Holocene formation of Leptosols, Regosols, Cambisols and Stagnic Cambisols. The areas of the lower limestone formation (mu) which weathered to a fine grained silty substrate and which lie in higher elevated areas and basins suffer equally

cc BY

common from surface gleying (Meynen, 1967). Because of Pleistocene solifluidal relocation processes compacted and impermeable soils developed which are widespread and further surface gleying. From an agricultural point of view, these soils are only arable when meliorated sufficiently (Schröder, 1983). The mean annual rainfall for this basin is about 800 mm/y. The used geological map for the Zemmer basins was the map of the south Kyll-Valley on a scale of 1:25 000 (Negendank and Wagner, 1988).

3 Methodology

Two model approaches based on dominant runoff processes with respect to regionalization were developed and compared to a reference map. Schobel (2005) generated this reference map based on the method of Scherrer and Naef (2003) during an intensive field campaign. In the two sub-basins of the Zemmer basin 15 representative soil profiles holding information on soil type, soil structure and soil physical properties and an additional 728 soil drilling points were available (see Fig. 1) for integration into modelling dominant runoff processes. Furthermore, 16 rainfall simulations in the two sub-basins provided an additional basis for determining the dominant runoff processes in the Zemmer basin (Müller, 2007, 2008).

3.1 Approach 1

Approach 1 makes use of a simplification of the procedure developed by Scherrer (1997), Scherrer and Naef (2003) and Scherrer (2006), because the original procedure requires extensive field campaigns and detailed soil maps, which are often not available for GIS-scale basins. The simplification assumes that the DRPs are mainly dependent on slope and the permeability of the substratum. For the simplified approach only a DEM, a geological and a land-use map are required as data input. Figure 2a schematically depicts this approach.

The first processing step is to generate the slope classes as defined by Scherrer

(PBS, 2006) from the DEM. The slope classes are: 0–3%, 3–5% 5–20% and >20%. However, one has to note that the classification according to Scherrer and Naef (2003) and Schobel (2005) was adapted to allow for comparing both approaches. Therefore, a fifth class is added (20–40%). Furthermore, based on the DEM GIS analyses are carried out to generate basin boundaries and the stream network. As a second step, the geological substrata of the basins are classified. This classification, which is based on the assessment of the permeability as suggested by Zumstein et al. (1989), who classified the infiltration permeability of the substratum with respect to its lithology and geo-hydrological characteristics such as fractures and porosity obtaining eight different permeability classes. The classification of Zumstein et al. (1989) was adapted and simplified into only two classes: permeable and impermeable. Table 2 lists the DRP dependency for forest, grass- and cropland with respect to slope and permeability as assumed in this study and used for the GIS analysis.

As a last step, the permeability layer is linked to the slope classes and the existing land-use map to determine a dominant runoff process for each of the polygons. The result will be a GIS-model that depicts the spatial distribution of the DRPs. Besides these previously defined criteria, a few additional assumptions have to be made and applied in the analysis. For urban areas, the DRP is supposed to be D_{HOF}, independent of permeability and slope. Furthermore, the D_{SOF1} process is assumed to have a very strong resemblance to D_{HOF} and occurs (often) only in near stream areas. Consequently, the stream network assigned a D_{SOF1}-area, identifying the area of the stream floodplain that saturates the quickest, depending on the location within the relief. The result of Approach 1 is a GIS-based model, reflected in the so-called GIS-DRP map and compared to the reference map (Schobel, 2005).

3.2 Approach 2

Approach 2 uses a statistical assessment of morphometric basin characteristics in order to model DRPs. For each DRP unit, which were mapped by Schobel (2005), the same set of morphometric basin characteristics is determined and by means of a

CC BY

Canonical Discriminant Analysis (CDA) an optimized separation of DRP units is obtained based on these characteristics. The results of the CDA is a set of functions and in compliance with these DRPs are modelled. The comparison of the modelled map with the reference map (Schobel, 2005) forms the basis of the quality control. The following chapters give a more detailed view of the process, which is also schematically depicted in Fig. 2b.

First, the reference map (Schobel, 2005) is crossed with the permeability of the substratum (see Approach 1) to differentiate between DRPs positioned on permeable and impermeable substratum, thus constructing two different discriminant models.

Next, a second data level was constructed, which consists of a DEM (resolution 20 m by 20 m, provided by the government of Rhineland Palatinate) and a set of derivates generated within the GRASS GIS 6.3.cvs (GRASS Development Team, 2008) software paket. The derivates describe the morphology and the slope segments of the sub-basins by attributing the following morphological characteristics: slope (degrees), aspect (degrees from east, counter clock-wise), profile curvature (in slope direction), tangential curvature (curvature parallel to the contour line), first and second order partial derivates in x and y direction as well as the flow path length and flow path density (up- and down slope). Additionally, the topographical index and its first and second order partial derivates in x and y direction as well as the steepness (S) and slope length (LS) factors were calculated.

To determine the terrain attributes of the different DRP units a univariate descriptive statistics procedure was applied to each of the DRP units, which includes the calculation of the number of raster cells in each DRP polygon (n) as well as the calculation of minimum, maximum, range, mean, standard deviation, variance, coefficient of variation and the sum of all values corresponding to each raster map generated as derivate of the DEM. This data is transformed into a table and then transferred to a statistical package (SPSS 15.0) for further analysis.

After exclusion of the areas with D_{HOF1} (these areas are considered to be mainly determined by buildings and other soil sealing features), 639 data sets will be analyzed

HESSD
5, 1677–1704, 2008

within the impermeable substratum group and 119 within the permeable substratum group. For both areas, a CDA is performed independently, considering an exclusion of parameters when the partial F-value ranges between 2.71 (maximum for rejection) and 3.84 (minimum for admission).

Approach 2 results in 2 statistical models, one for the impermeable and another for the permeable areas, in which the DRPs are described by 5 functions defined by the parameters included according to the conditions mentioned above. A cross-validation of the defined discriminant functions is performed, where each of the datasets is re-classified according to the defined models. The resulting map of DRPs based on the statistical analysis of the morphometric parameters is then compared with the results of the reference map (Schobel, 2005).

4 Results and discussion

4.1 Approach 1 (GIS-DRP)

The reference DRP map of the Zemmer basin and its two sub-basins (Grundsgraben and Schleidweiler) by Schobel (2005) is given in Fig. 3. Figure 4 shows the results of Approach 1 as the GIS-DRP map of the Zemmer basin.

The similarity between the GIS-DRP map and the reference map (Schobel, 2005) was a 77% at the Grundsgraben basin, with 8% of the total area only differing in one class (e.g. SSF2 instead of SSF3). At the Schleidweiler basin the similarity between the GIS-DRP and the reference-map was 82% (with 6% only differing in one class). The main difference between the maps was found for areas of the upper sandstone formation (so). This could be related to imprecise geological data input. A second but minor difference was observed for forested areas with a slope of 3–5%. In these areas D_{SSF3} was identified as dominant runoff process (see also Table 2) while D_{SOF2} occurred during intense rainfall events throughout several years of field observations (Schobel, 2005). The D_{SSF1} for cropland resulting from the newly introduced slope

CC BY

class 20–40% further weakened the similarity of the GIS-DRP map with the reference map. In order to remain as close as possible to the methodology of Scherrer and Naef (2003) this was tolerated. Near-stream areas also showed differences between the two maps. Due to the low resolution of the available DEM (20 m by 20 m) the width of the riparian zone, which produces D_{SOF1}, could not be determined with the basic settings of GIS-DRP. By classifying the riparian zone automatically as D_{SOF1} this problem can be solved, with the width now depending on the relief and its location within the stream network. For larger streams, this classification gave good results; however, for headwaters and accumulation in depressions no proper classification was achievable. Only more detailed data input (i.e. a higher resolution DEM or a field campaign) can solve this classification problem.

Impartial from the above-presented differences between both maps, the GIS-DRP map of the Grundsgraben and Schleidweiler sub-basins revealed a typical low mountain range distribution of dominant runoff processes. D_{SSF2} (46.1%) dominates in the Grundsgraben basin over D_{SOF2} (13.0%) and D_{DP} (12.9%). The Schleidweiler brook obtained the same results: D_{SSF2} (46.6%) against D_{SOF2} (17.8%) and D_{DP} (10.6%). Table 3 lists the distribution of the DRPs percentages for all basins.

4.2 Approach 2 (CDA-DRP)

Approach 2 resulted in two models comprised of the functions obtained through the canonical discriminant analysis: Table 4 lists the eigenvalues and canonical correlations of these functions for both the impermeable and permeable substrata while Table 5 lists canonical function coefficients of the discriminant functions for both substrata.

The discriminant analysis of the areas with impermeable substratum led to five discriminant functions. The first function explained 62% of the dataset variability while the first three functions summarized explained 95.1%. The permeable substratum areas were also defined by 5 functions explaining the variability with a significant reduction of variables: the first function explained only 46.5% of the dataset variability while the three first functions summarized explained 96.3%.

CC BY

The set of variables for impermeable substratum was reduced to: slope steepness, profile curvature, down slope flow path density and flow path length, first and second derivate of the DEM in E-W direction, the same derivates of the topographical index as well as the S and LS factors according to the USLE. The functions 1 and 2 were mainly determined by the S and LS factors and to a minor extent by the slope of the mapped unit. The steepness of the slopes (represented in the slope, S and LS factors) influenced the classification most. This was not astounding since the mapping method of Scherrer and Naef (2003) separated the different DRPs by taking slope into account. All other parameters defining the discriminant functions were almost irrelevant, explaining only 5% of the datasets' variability. The discriminant functions defined the dominant runoff processes to different extends. For the permeable substratum, the parameters were reduced: only the topographical index, the upslope flow density and the flow length as well as the first derivate of the topographical index in N-S direction and the S factor remained (see Table 5). All parameters distinguished the different functions well. Additionally, those parameters related to contributing areas and their position within the slope gained weight. The geological structure of the Zemmer study area, where the permeable areas are found at the deeply incised lower valley parts, attributed this.

Table 6 lists the classification accuracy by cross-classification of the model combination (in ha) and of both models. For the impermeable substratum, the first three functions identified D_{DP}, D_{SOF1} and D_{SOF3} well. However, the group centroids of the areas with D_{SSF2}, D_{SSF3} and D_{SOF2} were very close to each other (see Fig. 5a and b).

The fourth and the fifth function introduced an acceptable identification of D_{SSF3}. The cross-classification results for the impermeable substratum showed correct classification for more than 70% of the area with D_{SOF3} and D_{SSF2}. In contrast, D_{SOF2} and D_{SSF3} were interchangeable, since the first one was only correctly classified for about 57% of the surface area and often falsely classified as D_{SSF3}. Similarly for 33% of its surface D_{SSF3} was classified as D_{SOF2}. False classification also resulted for a large proportion of D_{DP} (34% of its surface classified as D_{SSF2}). For the permeable substratum it was possible to classify D_{DP}, D_{SOF1} and D_{SSF3} with good results. Very weak results (correct classification on less than 50% of the mapped area) were obtained for the classification of D_{SOF2}, D_{SOF3} and D_{SSF2} (permeable substratum; see Table 6). Especially D_{SOF2} was to a great extent (70%) classified as D_{SSF2}.

Combining both canonical discrimination function systems led to a correct classification of about 80% of the basin area (error of 19.1%, see as well Table 6). D_{SOF3} gave the best classification results, with 81% of its surface area correctly classified. D_{SOF1} also gave good classification results, with 79% of its surface area correctly classified. D_{SSF2} attributed to the majority of falsely classified D_{SOF1} surface area (9%)D_{SSF2} obtained good classification results as well (74% of its surface area correctly classified) and D_{SSF3} attributed to a substantial amount (11%) of the falsely classified area. For 69% of its surface area D_{DP} was classified correctly and most of the falsely classified surface area could be attributed to D_{SSF2} (11%). For 63% of its surface area D_{SSF3} was classified correctly and most of the falsely classified surface area could be attributed to D_{SOF2} (33%). Classified correctly for only 54% of its surface area was D_{SOF2}, where a large majority was classified falsely as D_{SSF3} (23%).

Both statistical models showed strongly differing model components and classification quality when compared to the reference map (Schobel, 2005). A different distribution of DRPs for each of the permeability sub-groups caused this. This was especially the case for the processes D_{SOF2}, D_{SOF3} and D_{SSF3}, which were represented for an area characterized by permeable substratum with less than 8 ha each (for a total surface area of 14 km^2). The classification accuracy of the processes was very low for this area. Furthermore, the two domination runoff processes with the lowest retrieval were interchangeably misclassified and therefore, topographical parameters cannot differentiate these different dominant runoff processes.

5 Conclusions

The objective of this study was to model dominant runoff production processes with a respect to regionalization. Two approaches were developed and their results compared to an existing dominant runoff processes reference map. The first approach constituted the emulation of a simplified derivation of runoff processes, using a modified approach of evaluating permeability of substratum in combination with slope and land-use classification. The second, statistical, approach used the derivates of a DEM as variables defining the different dominating runoff production process areas. For this purpose, a canonical discriminant analysis was used to build the model for derivation of homogeneous process areas.

The first approach was able to specify the DRPs for the experimental Zemmer micro-scale basin with an acceptable level of accuracy. This indicated that the approach could very well be used as an alternative to extensive measurement campaigns in order to define the dominating runoff production processes. The largest uncertainties were attributed to coarse geological mapping, low resolution of the DEM and the misinterpretation of D_{DP} and D_{SOF1} in the riparian zone.

The second approach showed clearly a strong dependency of the modelled DRPs on the topography of the Zemmer basin. The low occurrence of some of the DRPs for different types of permeability mainly attributed to uncertainty, which made the statistical classification weak. The dominant runoff process differentiation was strongly dependent on shape and position of the slope, soils and soil toposequences.

Modelling dominant runoff processes at the micro-scale the two approaches provided acceptable accuracy. The regionalization of both approaches at the meso-scale for mapping dominant runoff process, to be used in hydrological models, is the focus of further studies in the Rhineland Palatinate (Germany) and the Grand Duchy of Luxembourg.

Acknowledgements. This study was carried out in the framework of the WaReLa INTERREG IIIB project and ForeSTClim INTERREG IVB project.

References

Anderson, M. G. and Burt, T. P.: Process Studies in Hillslope Hydrology, John Wiley & Sons, Chichester, 1–8, 1990.

Blöschl, G.: Scale and scaling in hydrology, Wiener Mitteilungen, Wasser-Abwasser-Gewässer, Wien, Österreich, p. 162, 1996.

Buttle, J. M. and McDonald, D. J.: Coupled vertical and lateral preferential flow on a forested slope, Water Resour. Res., 38, No. 5, 18–1–17, doi:10.1029/2001WR000773/2002, 2002.

Faeh, A. O.: Understanding the processes of discharge formation under extreme precipitation – A study based on the numerical simulation of hillslope experiments, Mitteilung der Versuchsanstalt für Wasserbau, Hydrologie und Glaziologie, ETH Zürich, 150 pp., 1997.

GRASS Development Team: Geographic Resources Analysis Support System (GRASS) Software, Version 6.3.0. http://grass.osgeo.org, 2008.

Hellebrand, H., Hoffmann, L., Juilleret, J., and Pfister L.: Assessing winter storm flow generation by means of permeability of the lithology and dominating runoff production processes, Hydrol. Earth Syst. Sci., 11, 1673–1682, 2007, http://www.hydrol-earth-syst-sci.net/11/1673/2007/.

Kravchenko, A. N., Bollero, G. A., Omonode, R. A., and Bullock, D. G.: Quantitative Mapping of Soil Drainage Classes Using Topographical Data and Soil Electrical Conductivity, Soil Sci. Soc. Am. J., 66, 235–243, 2002.

McDonnell, J. J.: Where does water go when it rains? Moving beyond the variable source area concept of rainfall-runoff response, Hydrol. Processes, 17, 1869–1875, 2003.

McDonnell, J. J.: A rationale for old water discharge through macropores in a steep, humid catchment, Water Resour. Res., 26, 2821–2832, 1990.

Meynen, E.: Das Bitburger Land, in: Forschungen zur Deutschen Landeskunde, vol. 26, 2nd Ed., Bad Godesberg, 1967.

Montgomery, D. R., Dietrich, W. E., Torres, R., Anderson, S. P., Heffner, J. T., and Loague, K.: Hydrologic response of a steep, unchanneled valley to natural and applied rainfall, Water Resour. Res., 33(1), 91–109, 1997.

Müller, C., Sauer, T., Schneider, R., Schröder, D.: An integrative agricultural management approach to improving flood protection in agricultural areas, in: Integrated catchment management for hazard mitigation, edited by: Schüler, G., Proceedings of the 1st Scientific Conference, Trier and Trippstadt, 47–50, 2007.

CC BY

[1]

Negendank, J. F. W. and Wagner, W.: Geologische Karte 1:25 000 Trinkwasserprojekt Kylltal, Blatt Süd, Universität Trier, 1988.

Peschke, G., Etzenberg, C., Töpfer, J., Zimmermann, S., and Müller, G.: Runoff generation regionalization: analysis and a possible approach to a solution, IAHS Publ. 254 (Regionalization in Hydrology), 147–156, 1999.

Scherrer, S.: Abflussbildung bei Starkniederschlägen, Identifikation von Abflussprozessen mittels künstlicher Niederschläge, VAW – Versuchsanstalt für Wasserbau, Hydrologie und Glaziologie der ETH Zürich, Zürich, 147 pp., 1997.

Scherrer, S. and Naef, F.: A decision scheme to identify dominant flow processes at the plotscale for the evaluation of contributing areas at the catchment-scale, in: Runoff generation and implications for river basin modelling, edited by: Leibungut, C., Uhlenbrook, S. and McDonell, J., Freiburger Schriften zur Hydrologie, 13, 11–16, Freiburg, Germany, 2001.

Scherrer, S. and Naef, F.: A decision scheme to identify dominant flow processes at the plotscale for the evaluation of contributing areas at the catchments-scale, Hydrol. Process., 17(2), 391–401, 2003.

Scherrer, S.: Bestimmungsschlüssel zur Identifikation von hochwasserrelevanten Flächen. LUWG, Bericht 18, Mainz, 1–126, 2006.

Schmocker-Fackel, P., Naef, F., and Scherrer, S.: Identifying runoff processes on the plot and catchment scale, Hydrol. Earth Syst. Sci., 11, 891–906, 2007, http://www.hydrol-earth-syst-sci.net/11/891/2007/.

Schobel, S.: Erläuterungsbericht zur Abflussprozesskarte der Einzugsgebiete des Grundgrabens und Schleidweiler Baches bei der Gemeinde Zemmer/Eifel: Ber. f. d. Forschungsanstalt für Waldökologie und Forstwirtschaft Rheinland-Pfalz, Trippstadt, 2005.

Schröder, D.: Böden des Trierer Raums – Mitteilungen der Deutschen Bodenkundlichen Gesellschaft, 37, 159–284. 1983.

Sinowski, W. and Auerswald, K.: Using relief parameters in a discriminant analysis to stratify geological areas with different spatial variability of soil properties, Geoderma 89, 113–128, 1999.

Ticehurst, J. L., Cresswell, H. P., McKenzie, N. J., and Glover, M. R.: Interpreting soil and topo-

[1] Müller, C.: Hochwasserschutz in der Landwirtschaft – Validierung und Modellierung ausgewählter Maßnahmen, Dissertation, Universität Trier, in preparation, Trier, 2008.

graphic properties to conceptualise hillslope hydrology, Geoderma, 137, 279–292, 2007.
Walter, R.: Geologie von Mitteleuropa, 6. Aufl., Stuttgart, 1995.
Weiler, M. and Naef, F.: Simulating surface and subsurface initiation of macropore flow, J. Hydrol., 273, 139–154, 2003.
Weiler, M., McDonnell, J. J., Tromp-van Meerveld, I., and Uchida, T.: Subsurface Stormflow, in: Encyclopedia of Hydrol. Sci., Chapter 112, edited by: Anderson, M. G. and Mc-Donnell, J. J., John Wiley & Sons, Ltd., 1719–1733, 2005.
Zumstein, J. F., Gille, E., Decloux, J. P., and Paris, P.: Atlas de la lithologie et de la perméabilité du bassin Rhin-Meuse, Agence de l'Eau Rhin-Meuse, Moulin-les-Metz, France, 1989.

HESSD
5, 1677–1704, 2008

HESSD

5, 1677–1704, 2008

Modelling dominant runoff processes at the micro-scale

C. Müller et al.

CC BY

Table 1. Physiographic basin characteristics of the Zemmer sub-basins Grundsgraben and Schleidweiler, Germany.

Basin	Area	Land-use Urban	Land-use Forest	Land-use Grassland	Land-use Cropland	Substratum Permeable	Substratum Impermeable	Slope 0–3	Slope 3–5	Slope 5–20	Slope 20–40	Slope >40
	[km^2]	[%]	[%]	[%]	[%]	[%]	[%]	[%]	[%]	[%]	[%]	[%]
Grundsgraben	9.67	11	24	17	48	16	84	13	21	53	8	6
Schleidweiler	4.29	13	35	29	23	23	77	6	18	63	6	7

Table 2. The assumed dependency of the dominant runoff production processes on slope and permeability of the substratum for cropland, grassland and forest.

Slope [%]	Impermeable substratum Grass-and cropland/forest	Permeable substratum Grass-, cropland and forest
0–3	D_{SOF3}	D_{DP}
3–5	D_{SOF2}/D_{SSF3}	D_{DP}
5–20	D_{SSF2}	D_{DP}
20–40	D_{SSF1}/D_{SSF2}	D_{DP}
>40	D_{SSF1}	D_{DP}

HESSD

5, 1677–1704, 2008

Modelling dominant runoff processes at the micro-scale

C. Müller et al.

Table 3. Dominating Runoff Processes (DRPs); class of risk 1–5 by GIS-DRP-approach (1 relatively most abruptly changing flow reaction and 5 the most gradually changing flow reaction).

Class of risk	Grundsgraben	Schleidweiler
1	12.6	13.3
2	16.0	7.4
3	46.1	46.6
4	12.5	14.9
5	12.8	17.8

HESSD

5, 1677–1704, 2008

Table 4. Eigenvalues and canonical correlations of the discriminant functions of both models.

	Impermeable substratum			Permeable substratum		
Function	Eigenvalue	Cumulated variance [%]	Canonical correlation	Eigenvalue	Cumulated variance [%]	Canonical correlation
1	1.6806	61.9	0.7918	1.2576	46.5	0.7464
2	0.5483	82.2	0.5951	1.0980	87.1	0.7234
3	0.3519	95.1	0.5102	0.2495	96.3	0.4469
4	0.0724	97.8	0.2598	0.0933	99.7	0.2921
5	0.0598	100.0	0.2376	0.0073	100.0	0.0849

HESSD
5, 1677–1704, 2008

Table 5. Canonical function coefficients of the discriminant functions at the impermeable and permeable area.

		Functions				
	Variables*	1	2	3	4	5
Impermeable substratum	SLOPE.AVG	0.5247	0.3685	−0.1552	0.1943	0.0057
	SLOPE.cVAR	−0.0060	0.0511	0.0004	−0.0639	0.0431
	PROCURV.cVAR	−0.000011	−0.000018	0.000010	−0.000017	−0.000002
	FLDENS3D.MIN	0.0564	0.1878	0.1011	0.0633	0.0140
	FLDENS3D.STD	0.0007	0.0002	0.0059	0.0017	−0.0015
	FLENGTH3D.AVG	−00.0002	−0.0003	−0.0002	0.0015	0.0035
	DX.AVG	−5.7552	5.1703	−3.1945	7.1294	−5.4545
	DXX.MAX	−13.4348	−205.2000	−41.4345	−73.7205	−5.2724
	TOPDX.AVG	−3.5566	16.5336	21.1848	6.1902	8.7817
	TOPDXX.VAR	161.55	12.05	21171.31	22095.43	−2892.46
	LS.AVG	−0.0717	0.0490	0.0027	0.0009	0.0117
	S.AVG	0.1777	-0.1791	0.0208	-0.0445	0.0121
	Constant	−3.1823	−0.1829	−0.4129	0.7810	−3.5005
Permeable substratum	TOPIND.AVG	−0.373556	0.501012	0.077939	0.353923	0.349749
	uFLDENS3D.AVG	−0.001065	−0.001092	0.013130	−0.007205	0.007765
	FLENGTH3D.AVG	0.003433	0.003934	−0.002401	−0.000831	−0.001194
	TOPDY.MIN	10.678441	−3.529405	3.672470	15.916515	8.345410
	S.cVAR	−0.001162	0.012003	0.016723	0.018129	−0.018287
	Constant	2.545873	−5.973161	−0.727873	−2.422493	−1.393559

* The variables are composed as follows: SLOPE=slope in r; PROCURV=profile curvature; FLDENS3D=flowline density; FLENGTH3D=flowline length; DX=partial derivate of the DEM in x-direction; DXX=second partial derivate of the DEM in x-direction; TOPDX=partial derivate of the topographical index in x-direction; TOPDXX=second partial derivate of the topographical index in x-direction; LS=LS-factor from USLE; S=S-factor from USLE; TOPIND=topographical index; uFLDENS3D=flowline density oriented upslope; TOPDY=partial derivate of the topographical index in y-direction. The second part of the variable abbreviated as follows: AVG=average; cVAR=coefficient of variation; MIN=minimum; STD=standard deviation; MAX=maximum.

CC BY

Table 6. Classification accuracy by cross-classification of the model combination (in ha) and of both models at the area of Zemmer (in percentage of the mapped surface).

	Area [ha]	D_{SOF1}	D_{SOF2}	D_{SOF3}	D_{SSF2}	D_{SSF3}	D_{DP}
		Dominant Runoff Processes					
Model combinations	D_{SOF1}	58.9	4.0	0.3	6.9	0.9	1.8
	D_{SOF2}	8.	100.8	22.4	9.1	43.2	0.1
	D_{SOF3}	2.8	9.7	100.7	0.3	7.0	6.4
	D_{SSF2}	6.4	47.3	1.2	445.3	68.5	29.8
	D_{SSF3}	0.1	26.7	3.8	1.2	54.3	0.00
	D_{DP}	30.9	0.5	0.9	34.4	0.2	149.4
	%						
	D_{SOF1}	*79.2*	5.3	0.4	9.2	1.2	2.4
	D_{SOF2}	4.4	*54.1*	12.0	4.9	23.2	0.1
	D_{SOF3}	2.2	7.8	*81.1*	0.3	5.7	5.2
	D_{SSF2}	1.1	7.9	0.2	*74.3*	11.4	5.0
	D_{SSF3}	0.1	31.2	4.4	1.4	*63.3*	0.0
	D_{DP}	14.3	0.2	0.4	15.9	0.1	*69.1*
Impermeable substratum	D_{SOF1}	*64.0*	10.3	0.9	18.4	2.5	3.4
	D_{SOF2}	4.4	*56.6*	12.7	2.0	24.2	0.1
	D_{SOF3}	1.8	7.1	*85.5*	0.0	5.6	0.0
	D_{SSF2}	0.7	7.8	0.2	*75.7*	11.2	4.5
	D_{SSF3}	0.1	32.7	3.7	0.9	*62.6*	0.0
	D_{DP}	1.0	0.0	0.0	34.0	0.4	*64.6*
Permeable substratum	D_{SOF1}	*97.1*	0.7	0.0	0.6	0.0	1.6
	D_{SOF2}	5.8	*15.8*	0.0	70.2	8.2	0.0
	D_{SOF3}	11.2	23.9	*49.6*	5.0	10.2	0.0
	D_{SSF2}	9.9	11.1	46.3	*46.3*	17.1	15.7
	D_{SSF3}	0.0	0.0	18.3	10.3	*71.4*	0.0
	D_{DP}	19.5	0.3	0.6	8.8	0.0	*70.9*

HESSD

5, 1677–1704, 2008

Modelling dominant runoff processes at the micro-scale

C. Müller et al.

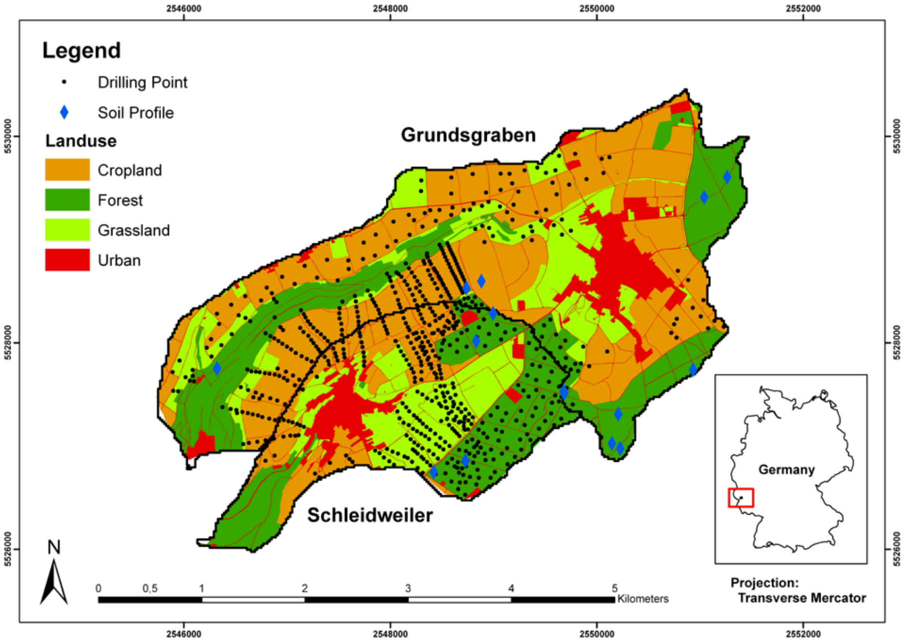

Fig. 1. Land-use map of the micro-scale experimental Zemmer basin (Germany) with the 15 soil profiles and 728 drilling points used for the reference map of Schobel (2005).

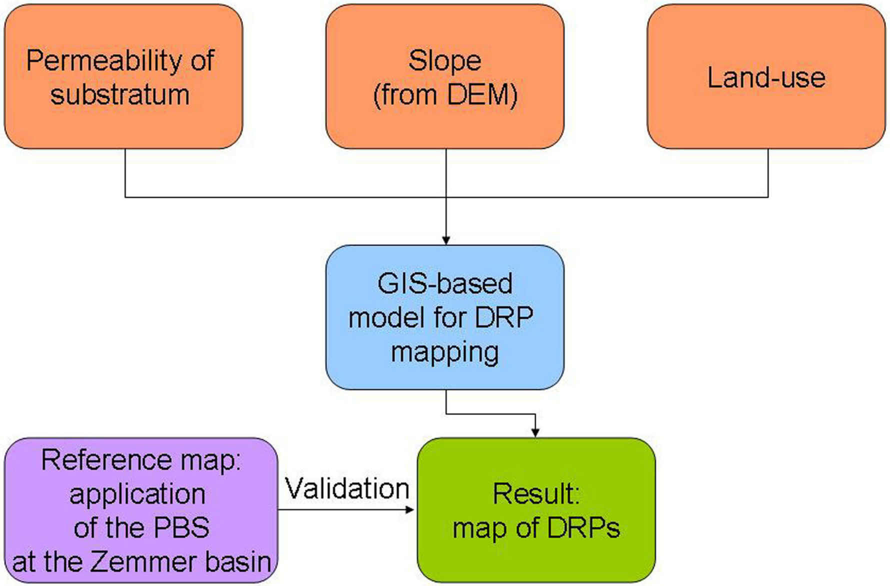

Fig. 2a. Schematic presentation of Approach 1, which assumes the dominant runoff processes depend on permeability of the substratum, slope and land-use.

HESSD
5, 1677–1704, 2008

Modelling dominant runoff processes at the micro-scale

C. Müller et al.

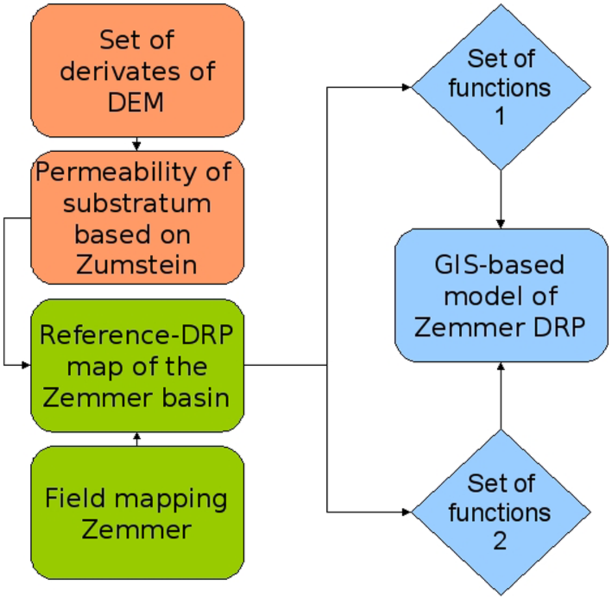

Fig. 2b. Schematic presentation of Approach 2, where the combination of a set of derivates of the DEM and the geology are used to discriminate the DRP units mapped in the field.

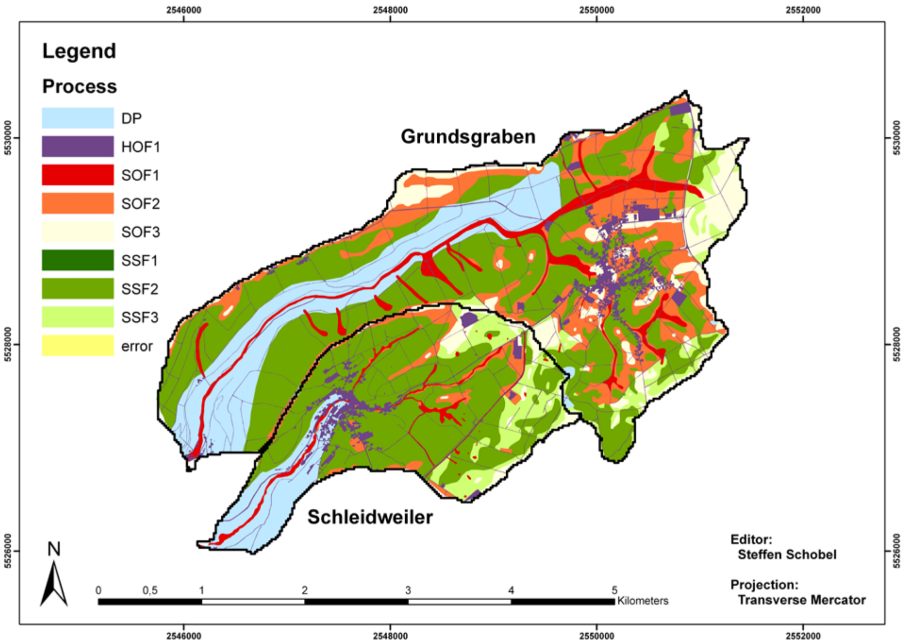

Fig. 3. Reference map of the dominant runoff processes as derived by Schobel (2005).

cc BY

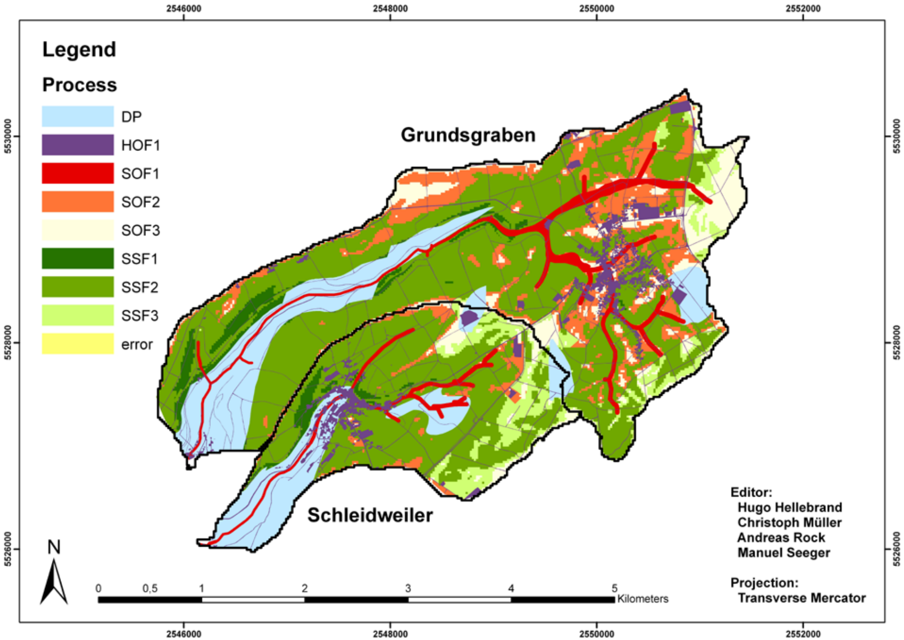

Fig. 4. GIS-DRP map of the dominating runoff processes for the Zemmer sub-basins Grundsgraben and Schleidweiler.

CC BY

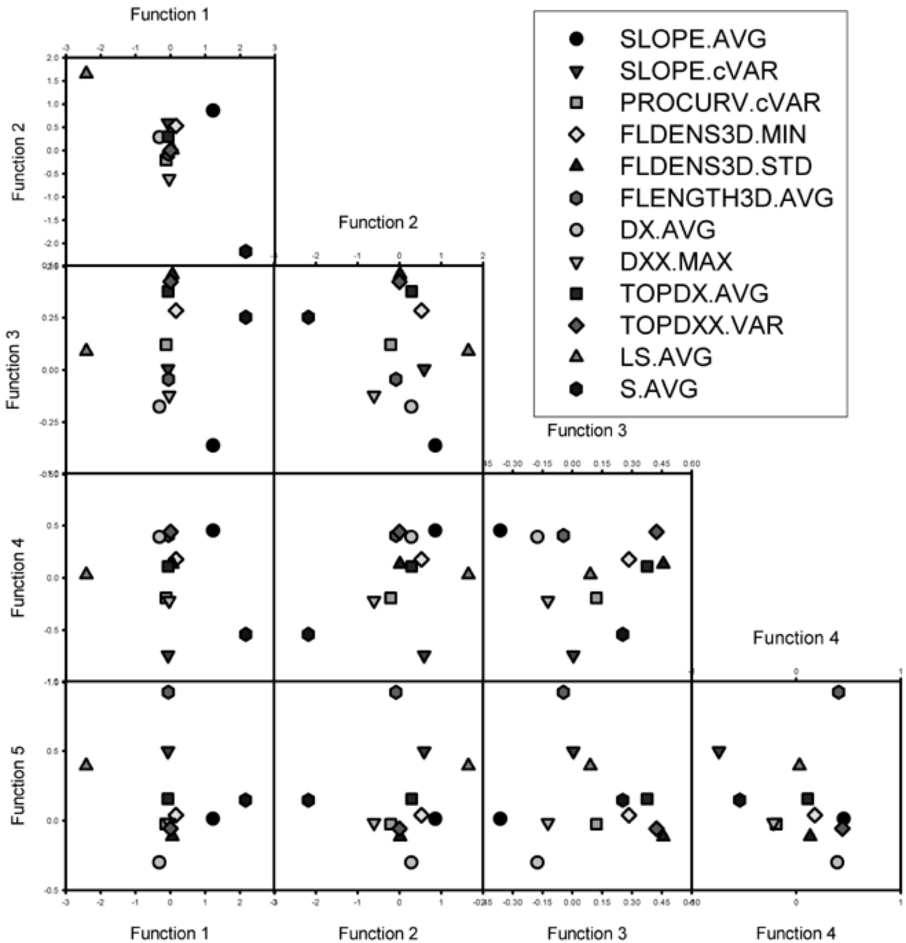

Fig. 5a. Weight of each variable within the discriminant functions for the impermeable **(a)** and permeable **(b)** area.

HESSD

5, 1677–1704, 2008

Title Page
Abstract | Introduction
Conclusions | References
Tables | Figures
◀◀ | ▶▶
◀ | ▶
Back | Close
Full Screen / Esc
Printer-friendly Version
Interactive Discussion

cc BY

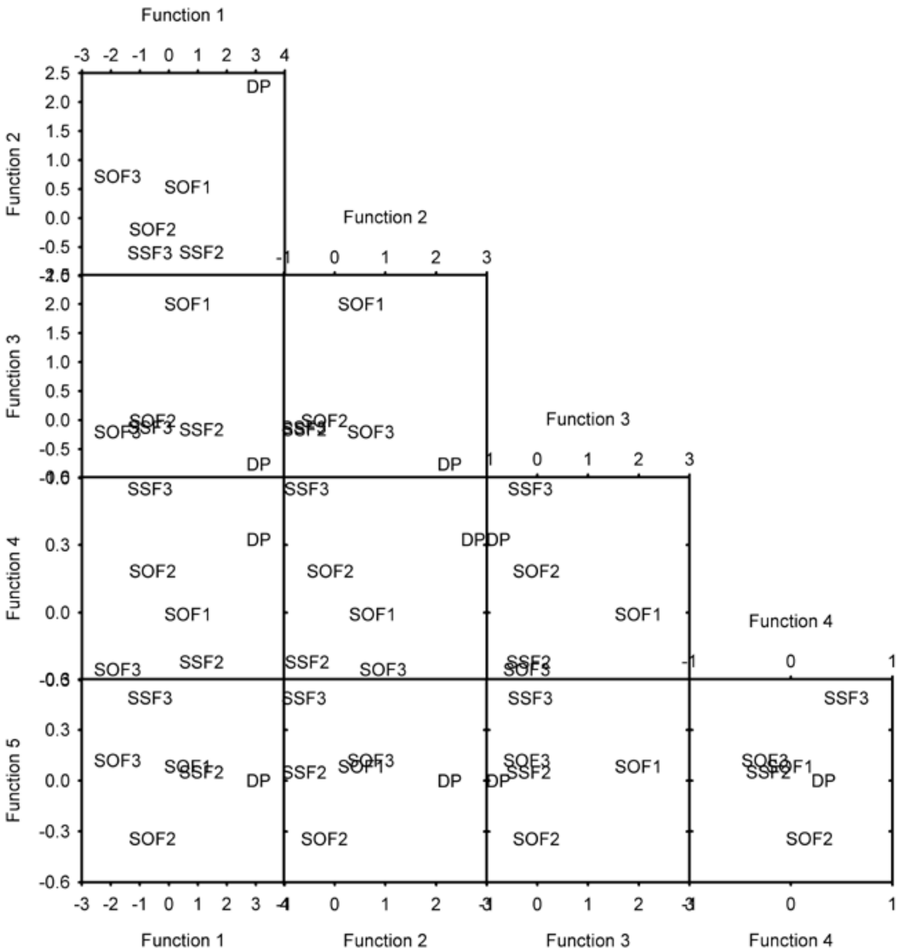

Fig. 5b. Centroids of DRPs within the impermeable substratum area.